

Article

Acid Leaching of La and Ce from Ferrocarbonatite-Related REE Ores

Diego Alejandro Tamayo-Soriano ¹, Ma. de Jesus Soria-Aguilar ^{2,*} , Nallely Guadalupe Picazo-Rodríguez ^{3,*},
Antonia Martínez-Luévanos ¹ , Francisco Raul Carrillo-Pedroza ^{2,*} , Ulises Figueroa-López ⁴
and Jesús Leobardo Valenzuela García ⁵ 

¹ Facultad de Ciencias Químicas, Universidad Autónoma de Coahuila, Saltillo 25280, Mexico; diegots88@gmail.com (D.A.T.-S.); aml15902@uadec.edu.mx (A.M.-L.)

² Facultad de Metalurgia, Universidad Autónoma de Coahuila, Monclova 25710, Mexico

³ Instituto Tecnológico Superior de Monclova, Tecnológico Nacional de México, Monclova 25701, Mexico

⁴ Escuela de Ingeniería y Ciencias, Tecnológico de Monterrey, Atizapán de Zaragoza 52926, Mexico; ufiguero@tec.mx

⁵ Departamento de Ingeniería Química y Metalurgia, Universidad de Sonora, Hermosillo 83290, Mexico; jesuleobardo.valenzuela@unison.mx

* Correspondence: ma.soria@uadec.edu.mx (M.d.J.S.-A.); nallely.pr@monclova.tecnm.mx (N.G.P.-R.); raul.carrillo@uadec.edu.mx (F.R.C.-P.)

Abstract: Rare earth elements comprise a group of 17 chemically similar elements, which increases the difficulty of separating them by traditional methods. For this reason, hydrometallurgy has been the most used method. However, it is important to evaluate the efficiency of the leaching processes used because, in addition to depending on the operating parameters of the leaching, they also depend on the mineralogical composition of the sample. In the present work, the extraction of Ce and La contained in the ferrocarbonatite mineral from the north of Mexico was studied. For the leaching tests, several leaching agents were used (HCl, H₂SO₄, HNO₃, and H₃PO₄ in different concentrations (0.5 [M], 1 [M], 1.5 [M]) and the temperature was modified to 20, 40, and 60 °C. A maximum recovery of 70% for Ce and La was obtained using HCl 1M in 4 h. The results of the kinetic study of the experiments showed that the best fitting model according to these kinetic models was the SCM controlled by a chemical reaction.

Keywords: leaching; kinetics; lanthanum; cerium; ferrocarbonatite ores



Citation: Tamayo-Soriano, D.A.; Soria-Aguilar, M.d.J.; Picazo-Rodríguez, N.G.; Martínez-Luévanos, A.; Carrillo-Pedroza, F.R.; Figueroa-López, U.; Valenzuela García, J.L. Acid Leaching of La and Ce from Ferrocarbonatite-Related REE Ores. *Minerals* **2024**, *14*, 504. <https://doi.org/10.3390/min14050504>

Academic Editor: George Blankson Abaka-Wood

Received: 22 March 2024
Revised: 30 April 2024
Accepted: 8 May 2024
Published: 10 May 2024



Copyright: © 2024 by the authors. Licensee MDPI, Basel, Switzerland. This article is an open access article distributed under the terms and conditions of the Creative Commons Attribution (CC BY) license (<https://creativecommons.org/licenses/by/4.0/>).

1. Introduction

According to Ford et al. (2023), rare earth elements consist of a group of 15 elements (La, Ce, Pr, Nd, Pm, Sm, Eu, Gd, Tb, Dy, Ho, Er, Tm, Yb, Lu, Y, and Sc) which are classified into light rare earths (LREE), from La to Gd, and heavy rare earths, which include elements from Tb to Lu plus Y. According to these researchers, rare earths are considered critical metals, and their production is necessary for a low-carbon economy to be established, since among the applications of this type of metals is the manufacture of batteries [1].

REEs represent around 0.015% of the composition of the Earth's crust, with average values ranging from 10 to 500 ppm. Although they exist in abundance in the Earth's crust, their respective levels of concentration constitute an important limiting variable for developing economically feasible exploitation. The United States Geological Survey, the principal compiler of data on the REEs, estimates that worldwide reserves total some 120 million tons. China has the largest reserves, approximately 37%, followed by Brazil and Vietnam, each with 18%, Russia with 15%, India with around 6%, Australia with 3%, and the U.S. with 1% [2]. Of these reserves, the majority of global REE production currently comes from four minerals: bastnäsite, monazite, xenotime, and loparite. In China, bastnäsite constitutes the largest percentage of global REE production, followed by

monazite in Australia and India, loparite in Russia, and xenotime in Malaysia. These rare earth-containing minerals are mainly associated with igneous rocks (alkaline rocks and carbonatites) [3].

As mentioned earlier, China is the main producer of REE worldwide since it produces more than 60% of these metals from deposits that are related to carbonatite, an element which also contains metals considered critical, such as Nb, Th, and Sc. According to researchers, carbonatite deposits can be divided into three types: primary magmatic, hydrothermal type, and eroded carbonatite crust type [4]. The carbonatite deposits contain at least 15 different earth minerals identified as silicocarbonatite, magnesiumcarbonatite, ferrocyanatite, and calciumcarbonatite, among others, which are concentrated by flotation with acid-based collectors [5].

Some researchers have established that the enrichment of REE in these mineral species is due to the fractional crystallization of large amounts of calcites, which are incompatible with REE, associated with barite and alkaline silicates [6].

Carbonatite deposits generally contain high concentrations of LREE; some researchers have reported carbonatite deposits with high concentrations of Fe and LREE [7]. When carbonatite is rich in iron, it is called ferrocyanatite [8]. Derived from the above, some researchers have reported that iron has a negative effect during the leaching processes of rare earths, which is why it is important to study the influence of iron in leaching systems [9].

Regarding their properties, the REEs appear together in nature due to their similar physicochemical characteristics: except for Ce^{+4} and Eu^{+2} , which have similar ionic radius, they are all trivalent ions (state of oxidation +3). This similarity allows for some REEs to be substituted for others in certain crystalline networks. This explains why multiple elements of this group may be present in the same mineral ore. This set of chemical elements has specific magnetic, optical, and conductive properties that make them unique and, for this reason, coveted by modern industry [10].

REEs belong to a group of elements that are very difficult to separate using traditional techniques because, as mentioned above, they possess such similar chemical properties. The method most used in recovery, then, involves hydrometallurgy [2]. This means that it is extremely important to evaluate the efficiency of the leaching processes utilized, as this depends largely on the precise mineralogical composition of the sample ore and related operative parameters, including the nature of the acid used, its concentration, temperature, reaction time, and the presence of impurities. The acids that can be utilized in decomposition processes include H_2SO_4 [11,12], HNO_3 [13], HCl [14], and H_3PO_4 [15].

Innocenzi and Veglió (2012) proposed a two-stage hydrometallurgical process for sequential leaching: the first stage is performed with H_2SO_4 at 2 [M], at a temperature in a range of 80–85 °C, and a time of 3 h. The second requires H_2SO_4 at 1 [M], at a temperature of 25 °C for one hour of contact. Extraction after running both stages can be as high as 99% of the REEs present in the ore. Selective precipitation with NaOH, adjusted to pH < 1.5, is used to obtain precipitated solids with recovery rates of REEs that approach 80% [16].

Studies by Kim et al. (2016) assessed the recovery process of lanthanum and cerium utilizing hydrochloric, sulfuric, and nitric acid. Their leaching tests revealed that the best agent for REEs is hydrochloric acid at ambient temperature and pressure, as recovery rates of 92 and 94% were registered [17]. Shen, Y., Jiang, Y., and Qiu, X. (2017), meanwhile, proposed a new and easier process for the selective leaching of trivalent REEs from the tetravalent cerium in the mineral bastnäsite. Their experiments explored the effects of acid concentration, leaching time, and temperature on the efficiency of leaching REEs from hydrothermally treated leached slag, followed by complete leaching with nitric acid at 4.0 mol/L. The specific surface area of the final leached slag was 57.7 m²/g, approximately 650 times greater than the brute mineral. Finally, they carried out selective leaching of RE (III) (>90%) without utilizing an organic dissolvent during extraction. There, the lowest Ce (IV) value occurred in the leached slag (>92%) [18].

Xu et al., 2019 studied the efficiency of extracting REEs from nitric acid leach solutions of phosphate ores using solvent extraction with a new amide extractant denominated TODGA. When the concentration of extractant increased to 0.1 mol/L, the extraction rates of lanthanum, cerium, praseodymium, and neodymium were found to be 98.1%, 99.1%, 98.8%, and 98.6%, respectively. The recovery rate reached 99.9% when a three-stage countercurrent extraction was carried out on the simulated leach solution. There was almost no extraction of other impurity ions, and the rare earths could be separated with TODGA from Ca^{2+} , Fe^{3+} , and Mg^{2+} [19].

Liu F., Porvali, A., Halli, P., Wilson, B., and Lundström, M. (2020) systematically analyzed and compared two processes. During the leaching stage, they studied the effect of increasing the concentrations of H_2SO_4 or HCl, determining that, while both can successfully promote the leaching of REEs, the HCl solutions extracted a broader range of metals. After leaching, they applied the oxalate and sulfate double precipitation methods to separate the REEs from the leached elements using HCl or H_2SO_4 . Their results suggest that they achieved precipitation rates of REEs < 99% with oxalate, but the purity of the products containing them was affected significantly by impurities like Fe and Co [20].

Echeverry Vargas, L. (2022) studied distinct leaching conditions with HCl and H_2SO_4 , attaining the maximum degree of extraction of cerium, lanthanum, and neodymium, and demonstrating that the highest extraction of these elements was accomplished with H_2SO_4 [21]. Table 1 presents the results of a literature review on the methods mentioned above for leaching processes based in acid to extract REEs.

Table 1. Leaching conditions using different aqueous solutions.

Solution	Concentration	Temperature, °C	Time, h	Reference
H_2SO_4	15%	100	2	[22]
HNO_3	3 M	25	8	[23]
HNO_3	2.5%	25	0.25	[24]
HCl	1.5 M	85	1	[25]
H_2SO_4		275	4.3	[26]
H_2SO_4	0.01 M	24	20–22	[27]
H_2SO_4	10%	2	20	[28]
H_2SO_4	1 g/L		24	[29]
H_2SO_4	10–30%	50	2	[30]
H_2SO_4	10%	60	1–2	[31]
HCl				
H_2SO_4	1.5 M	80	0.33	[32]
HNO_3				
HNO_3	36%	72		
H_2SO_4 and H_3PO_4	90–10%	72	1	[33]
HCl	2 M			
H_2SO_4	4 M	25	3	[34]

It is very important to mention that there are no research studies about Mexican REE deposits, and none related to leaching of REEs contained in Mexican ferrocarnatites.

In this context, research on the leaching of REEs (contained in Mexican ferrocarnatite ore) has focused on (1) determining the feasibility of treating this type of mineral through acid leaching and (2) evaluating, thermodynamically and kinetically, the Ce and La dissolution in these types of minerals.

Although La and Ce are the most abundant elements of REEs, their study has been increasing due to their applications in the manufacture of new alloys with high mechanical properties. Therefore, it is expected that the demand for La and Ce will continue to rise in the coming years [35,36]

Systematic studies of the kinetics of the leaching of REEs are, however, scarce, so it is necessary to explore this topic from both the mineralogical and kinetic perspectives during processes designed to leach REEs to increase leaching rates.

2. Materials and Methods

To carry out the tests, a mineral from the north of Mexico was used. It was ground in a ball mill (Model BINCO Inc., PO BOX 6339, North St Paul, MN, USA) and screened to obtain a particle size of less than 0.106 mm (Tyler 150 Mesh). After, a magnet was then used to separate the magnetic fractions containing ferromagnetic minerals from the paramagnetic and non-magnetic minerals containing the REEs. All particles were cleaned with deionized water. After each collection, non-magnetic particles were filtered, dried, and weighed for their respective content analysis of the elements of interest. Samples were analyzed using an energy dispersive XRF spectrometer to determine the percentage of REEs for the non-magnetic fraction obtained from the mentioned magnetic separation process.

The elemental chemical composition was determined using the X-ray fluorescence technique (XRF, Panalytical Epsilon) (Malvern Panalytical, Worcestershire, UK). This technique detects (in the equipment model used in this work) concentrations above 0.002%, with a precision of 0.001%. The presence of La and Ce was confirmed using a quadrupole mass spectrometer (QMS, Thermo iCAP Q) (Thermo Fisher Scientific, Waltham, MA, USA). The phases present in the mineral were determined using an X-ray diffractometer (XRD, Bruker D8) (Bruker, Billerica, MA, USA). Petrographic analysis was carried out by selecting representative rock samples of the mineral, and for this, a Carl Zeiss Axio Scope A.1 microscope (Carl Zeiss AG, Baden-Württemberg, Germany) was used. This step involved identifying the textural characteristics and alterations of the mineralogical species.

Leaching Tests

Three series of leaching tests were carried out using the non-magnetic fraction of the mineral. The experiments were carried out in Erlenmeyer flasks under magnetic stirring with an S/L (solid to liquid) ratio of 1/6 (50 g of sample in 300 mL of solution) and a stirring speed of 400 rpm.

The first series consisted of leaching experiments using different acid solutions (HCl, H₂SO₄, H₃PO₄, H₂SO₄ with HNO₃) at different molar concentrations (0.5, 0.5, 2.3, 0.5 + 0.1 M) for 1 h at room temperature. These concentrations were chosen within the range reported in the literature.

In the second series of experiments, the dissolution of Ce and La (Fe, Ca, and P) with respect to time was evaluated. In this series, only HCl and H₃PO₄ (both at 1 M) were used, since they are the ones that offered the best results in the first series.

The third series was carried out using only HCl at different temperatures (0, 20, 40 and 60 °C) in order to determine the activation energy in this aqueous medium.

3. Results and Discussion

3.1. Characterization

Table 2 shows the chemical analysis of the non-magnetic fraction sample used in this study. From the analysis, total element oxides for XRF in % and elements for QMS in ppm are reported.

Table 2. Chemical analysis of samples used in the experimental part.

		By XRF, %					By QMS, ppm	
FeO	CaO	SiO ₂	PO ₂	ZnO	CeO	LaO	Ce	La
30.09	12.55	9.04	2.35	1.79	0.253	0.163	2280	1470

It is important to mention that the non-magnetic fraction represents 50% of the sample. Even so, the high iron content indicates the presence of this element in the form of magnetite (magnetically separated) and other non-magnetic species such as hematite, goethite, or wustite. The content of Ce and La, in quantities that add up to a little more than 0.4%, are

equivalent to 4160 ppm or 4.16 kg/ton. It should also be mentioned that, in the previous balance, the non-magnetic fraction contains 80% of these rare earths.

To determine the mineral species present in the sample, X-ray diffraction analysis was carried out. The results are shown in Figures 1 and 2. Figure 1 shows the different mineral species of iron oxides. The analysis shows that the main phase present is wustite (FeO), also highlighting Fe-bearing (ferroan) dolomite and franklinite, and a presence of magnetite was also detected.

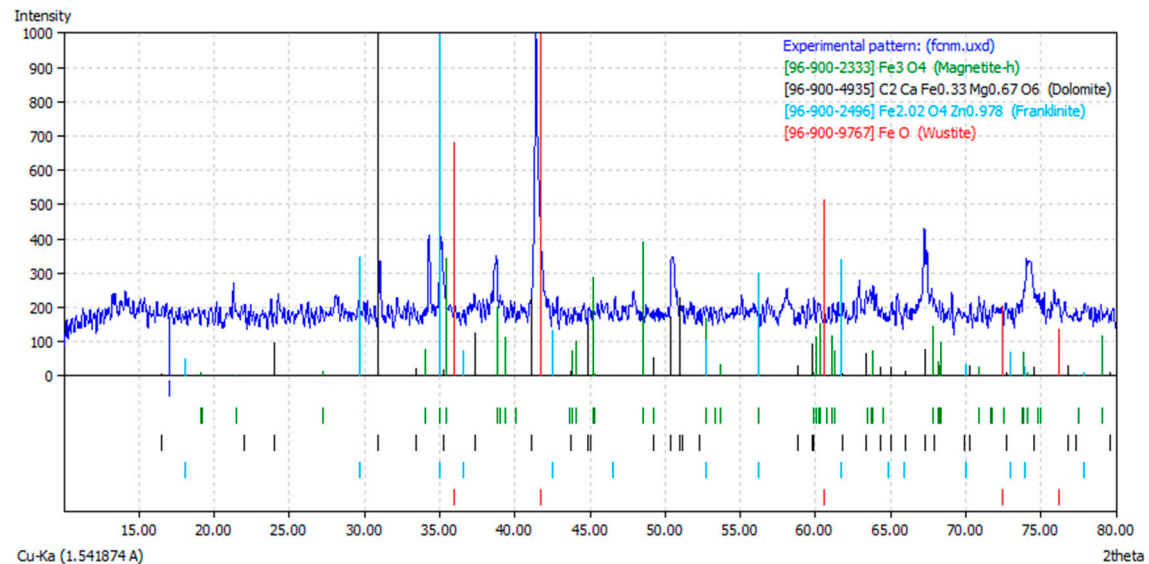


Figure 1. Diffraction patterns of the ore sample. Main iron mineral species.

Figure 2 shows other mineralogical species that contain the elements obtained in the XRF analysis. The main species detected were wollastonite, quartz, and the presence of apatite.

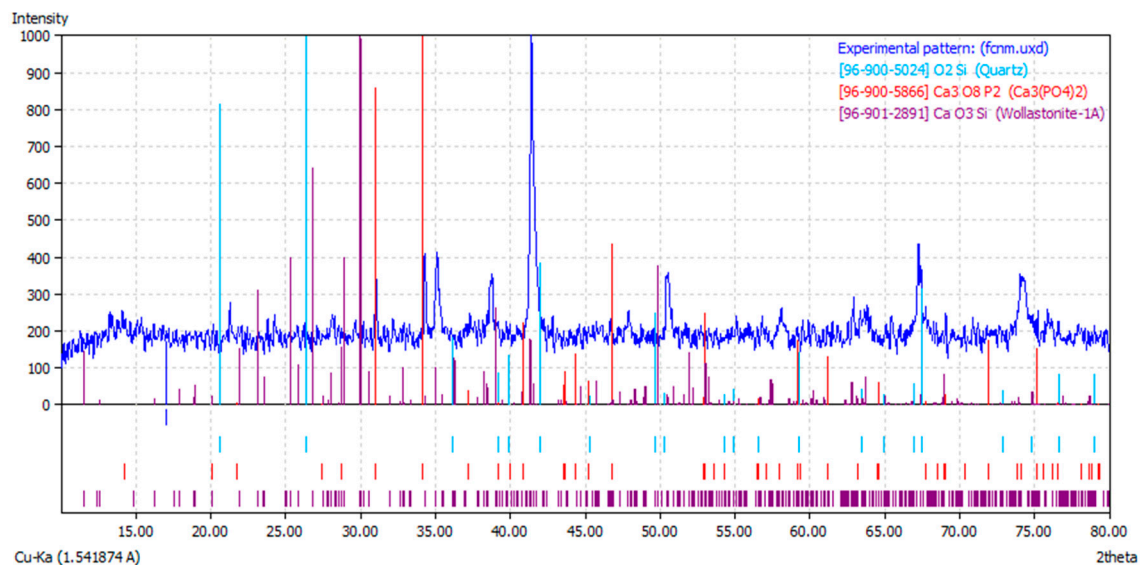


Figure 2. Diffraction patterns of the ore sample. Minor mineral species.

According to the literature, this type of mineral corresponds to a ferrocarnatite, where rare earth elements can be associated with phosphate-type minerals, such as apatite, in the form of monazite. To confirm the type of association of phosphates with other mineral rocks, the cleanest sample of iron oxides was obtained for petrographic analysis.

The petrographic analyses of the thin sections revealed predominant mineralogy. Observations included occasional euhedral and fibrous altered crystals. Figure 3 presents six microphotographs that correspond to the samples analyzed. From the optical perspective, all samples present similar characteristics. The relief is quite high, with a very low birefringence, interference colors up to first-order orange, and a parallel extinction. The analysis showed that they were biaxial with a negative optical sign. The 2 V angle oscillated from 36 to 60, and the extinction angle from 0 to 44. Alterations were observed mainly in the crystals rich in phosphates, likely due to the presence of apatite and/or monazite.

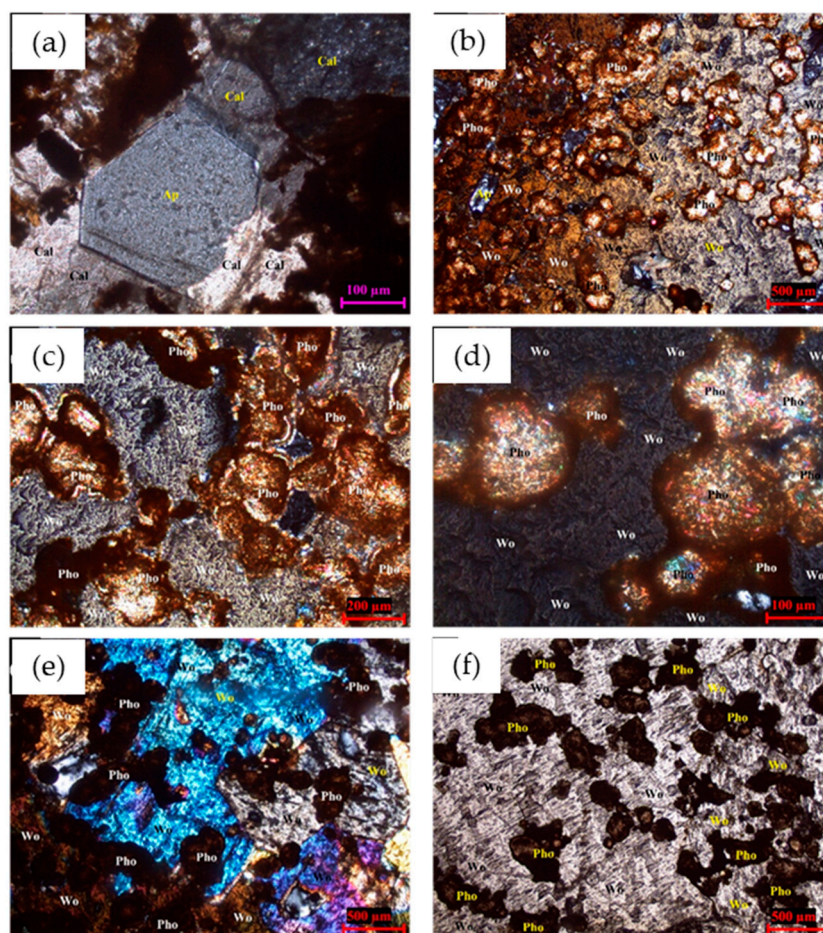


Figure 3. Photomicrographs of ferrockarbonatites, where a mineral composed mainly of wollastonite, phosphates, apatite, calcite and quartz is observed. Abbreviations: Wo = wollastonite; Ap = apatite; Pho = phosphates; Cal = calcite; Qz = quartz.

The optical characteristics observed under transmitted light petrographic microscopy made it possible to elucidate that the mineralization present was composed principally of altered wollastonite and phosphates (Figure 3a–f), with traces of calcite, quartzes, and opaque minerals. The petrographic analysis did not reveal the presence of mineral phases like granites, diopside, pectolite, or other minerals found in deposits of the Skarn type; thus, the proposal is that this mineralization is of magmatic origin, associated with alkaline magmatism in the study zone.

The phosphates of REEs form during the late stages of the hydrothermal process, in association with the generation of altered apatite (Figure 3a,b). These are, once again, phases rich in REEs, during which the separation of La and Ce occurs, forming small aggregates of cumulate texture [22]. These are very abundant minerals, usually of acicular shape, distributed in growing radials, very often associated with apatite or monazite (Figure 3b–d). In addition, the traces of apatite have been altered along the limits of their grain to form

an intergrowth type of corona made up of iron oxides (pale orange due to the alteration (Figure 3b).

Two types of apatite can be distinguished based on mineralogical studies:

Apatite 1: this type is found as intergrowth with magnetite. Euhedral crystals form; they can range in diameter from a few millimeters to a few centimeters. Their color generally appears to be yellow or light pink with different intensities. Only rarely are they seen to be pallid. This type correlates strongly with magnetite (Figure 3f).

Apatite 2: This apatite differs from Type I because its texture is finer and has less transparency and accumulation. Apatite II is characterized by very fine grains and a size that varies from 10 to 200 μm. This type occurs in the form of subhedral to anhedral crystals in the lenses with different-sized, thick veins that cut through the magnetite apatite mineral (see Figure 3a,b).

Considering the above, it is possible to deduce that the REEs (La and Ce) can be found hosted in apatite $C_{a5}(PO_4)_3(OH,F,Cl)$, partially replacing calcium within its crystalline structure, or perhaps in the form of monazite, $(Ce,La)PO_4$, associated or included in apatite. This type of association has been reported in carbonatite-type minerals [20].

3.2. Leaching

Leaching tests were carried out at distinct concentrations of HCl, H_2SO_4 , H_3PO_4 , and $H_2SO_4+HNO_3$. The objective was to determine the concentration most indicated for dissolving the REEs, as shown in Figure 4. The comparison of the leaching trials with the different acid solutions demonstrated that the best result was achieved with hydrochloric acid (HCl) at 1 M, as this produced over 50% extraction for both elements in a time of one hour. The findings further show that leaching with phosphoric acid (H_3PO_4) permitted obtaining extractions near 50%. However, this result was reached only at high concentrations of 2.3 M. The results of extraction with sulfuric acid were around 45%.

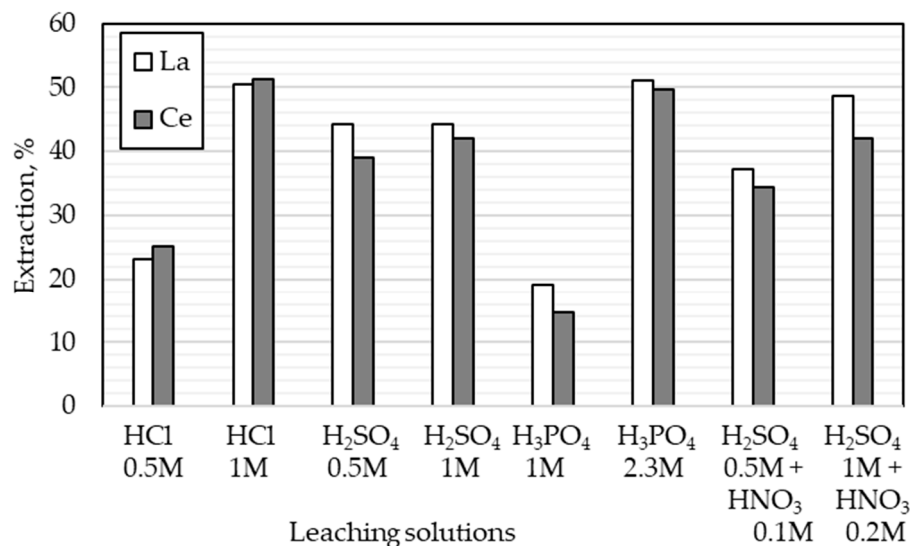
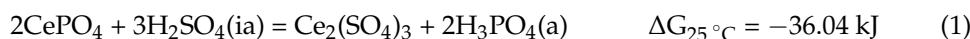
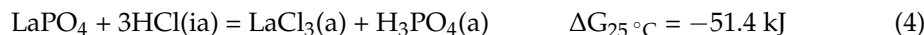
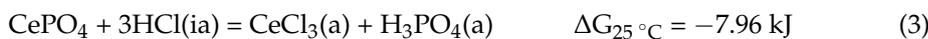


Figure 4. Extraction of La and Ce at different types of leaching solutions (temperature = 25 °C; leaching time = 1 h).

The principal reactions of the REEs with sulfuric acid during leaching are described below (reactions and Gibbs free energy obtained from HSC Software 6.1). Chemical compounds are considered simplified or separated from the formula of the mineral (apatite or monazite).



From the results, the major La and Ce quantity was dissolved when they were treated with HCl and H₃PO₄. According to HSC Software 6.1, the following chemical reactions can be proposed:



To determine which species can predominate under the conditions of the selected acids, predominance diagrams were obtained using the Medusa software version 2.2.5.2. Ce and La molar concentrations were used for diagram construction and calculated from the chemical analysis (Table 2) and experimental conditions (50 g in 300 mL) at 25 °C. Figure 5 shows the species of Ce and La in a 1 M HCl medium. In both cases, both Ce and La were found predominantly as CeCl²⁺ and LaCl²⁺ ions at acidic pH (less than seven).

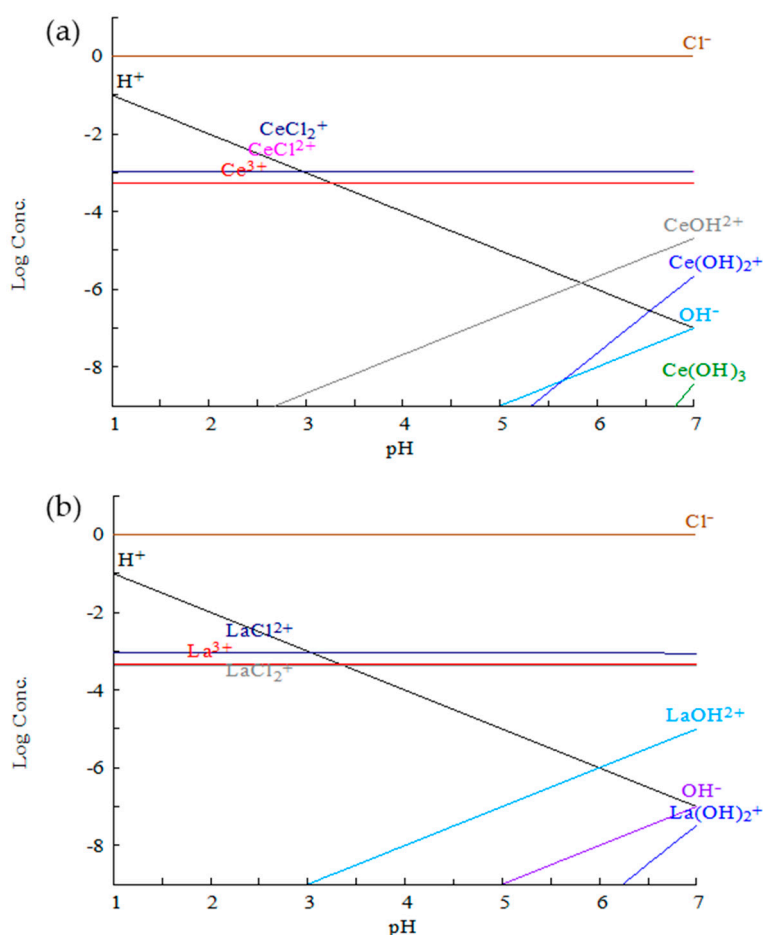


Figure 5. Predominance diagrams of (a) Ce and (b) La in a 1 M HCl aqueous medium.

So, the reactions can be rewritten as



Figure 6 shows the predominance diagrams for Ce and La using H₃PO₄. At pH of less than 1.5, the predominant species were Ce³⁺ and La³⁺. At pH between two and four,

the species were $\text{CeH}_2\text{PO}_4^{2+}$ and $\text{LaH}_2\text{PO}_4^{2+}$. Therefore, given that leaching ends at a pH of three for this medium, these species are present in the leaching solution. These species coincide with those shown in the reaction products of Equations (5) and (6).

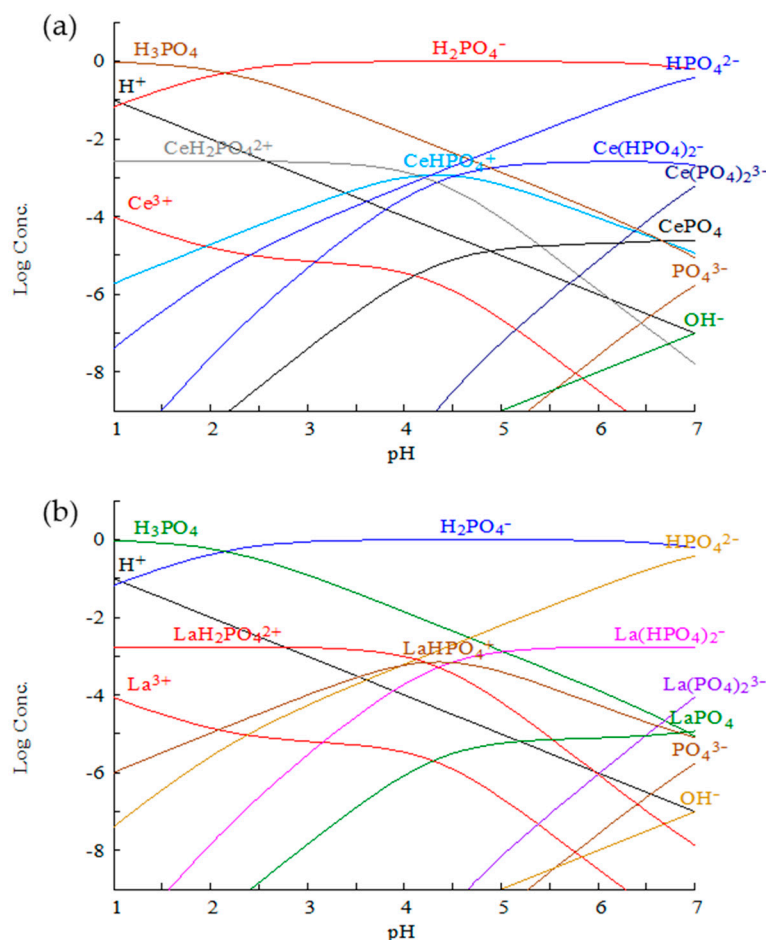


Figure 6. Predominance diagrams of (a) Ce and (b) La in a 1 M H_3PO_4 aqueous medium.

Therefore, according to the species distribution diagrams, the dissolution of La and Ce is thermodynamically possible under the acids considered in the present work and according to the works cited in the literature.

3.3. Kinetics

Extraction tests (in triplicate) were carried out with respect to time only for the two cases of the highest extraction observed in Figure 4, that is, H_3PO_4 and HCl. Figure 7 shows the extraction of the elements that make up the apatite with La and Ce and the behavior of Fe, with respect to time, using H_3PO_4 . The Ca and P curves follow the same trend until 180 min, reaching a dissolution of 95 and 75%, respectively. La and Ce dissolve following a similar trend until reaching an extraction of 47% at 180 min, after which it decreases. In the case of Fe, it is observed that it dissolves gradually, dissolving 16 and 28% at 180 and 240 min, respectively. The results indicate that phosphoric acid almost completely dissolves the compounds or mineral species that contain calcium (calcite, apatite, monazite). The achieved dissolution of 75% phosphorus extraction indicates the dissolution of the apatite and monazite species. The fact that only a 47% extraction of La and Ce has been achieved indicates that there is still undissolved monazite, and perhaps there is a presence of these rare earths in another mineral species less reactive to acid.

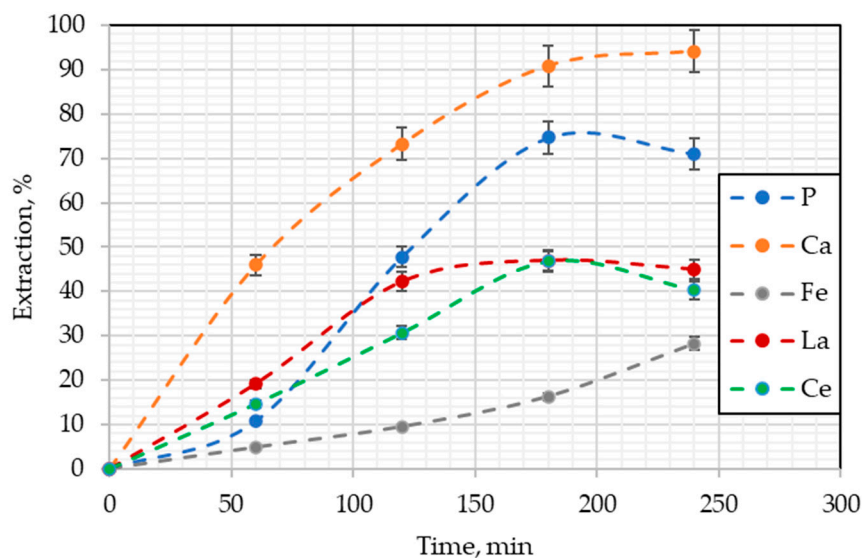


Figure 7. Leaching in a phosphoric acid medium ($H_3PO_4 = 1\text{ M}$; $T = 40\text{ }^\circ\text{C}$; $S/L = 1/6$).

Figure 8 shows the extraction behavior of the elements of interest using HCl. The Ca and P curves follow the same trend (similar slope), reaching a maximum extraction of 96 and 88% respectively, after 240 min of reaction. In the case of La and Ce, it is interesting to note that they practically have the same extraction behavior, and that both reach an extraction of 70% at 240 min. In the case of iron, the dissolution obtained was 20% at the mentioned time.

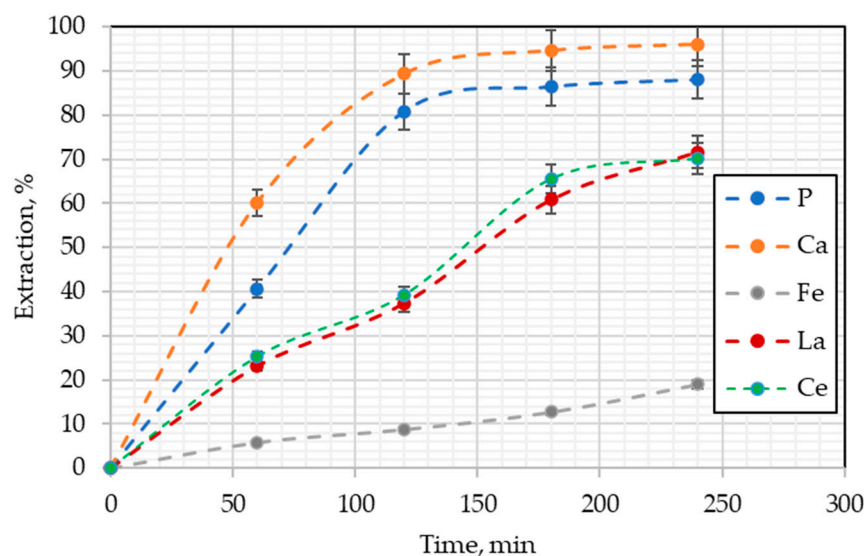


Figure 8. Leaching in a hydrochloric acid medium ($HCl = 1\text{ M}$; $T = 40\text{ }^\circ\text{C}$; $S/L = 1/6$).

These results show that hydrochloric acid can dissolve calcium species almost entirely; they also indicate a greater dissolution of phosphorus-containing species. Consequently, greater extraction of rare earths is obtained. On the other hand, the relatively low extraction of iron coincides with the slower dissolution of the predominant species of this element, hematite.

A kinetic analysis was conducted to determine the model that can best be applied to this process of mineral dissolution. The results of the chemical analyses obtained from the leaching experiments with respect to time were used to evaluate the kinetic models and determine the one with the best adjustment. Studying kinetic behavior or model is important for designing or broadening the leaching process, since it describes the

dissolution rates of phosphorous, calcium, iron, lanthanum, and cerium using solutions of hydrochloric (HCl) and phosphoric acids (H_2PO_3) as leaching agents.

Many authors assume that heterogeneous reaction kinetics for most of the metal's extraction process can be interpreted by using shrinking models. Of these, the shrinking core model (SCM) is the most used model for describing the kinetics in leaching processes [37–44]. In this case, the following steps are identified during the leaching: diffusion of the leaching agent through the thin liquid film surrounding the particle, diffusion of the leaching agent through the solid product layer, and reaction on the surface of the unreacted core. If there is a liquid product, it needs to be evacuated by diffusion through product layer and liquid film to the bulk of the liquid. As a result, three main mechanisms of liquid film diffusion, product layer diffusion, and chemical reaction affect the leaching kinetics [37,44].

In the case of present study, the mechanism of the heterogeneous reaction may take place as follows. Initially, the reactants (the acids) diffuse from the bulk of the aqueous phase to the interface between the aqueous phase and the solid (mineral sample). If an additional layer of inert material (iron oxides, mainly) is present at the interface, the reactants have to overcome the resistance of this layer before reaching the surface of the monazite (or apatite containing La and Ce).

As scanning electron microscopy (SEM) photographs show (Figure 9), the particle size maintains the same approximate value after the leaching reaction, assuming that these particles are mostly iron oxides (as indicated by chemical analysis) and that the minerals containing La and Ce are released. After 4 h, the EDS spot analysis indicates that there is no presence of said La and Ce minerals. Therefore, it is possible to affirm that they were dissolved.

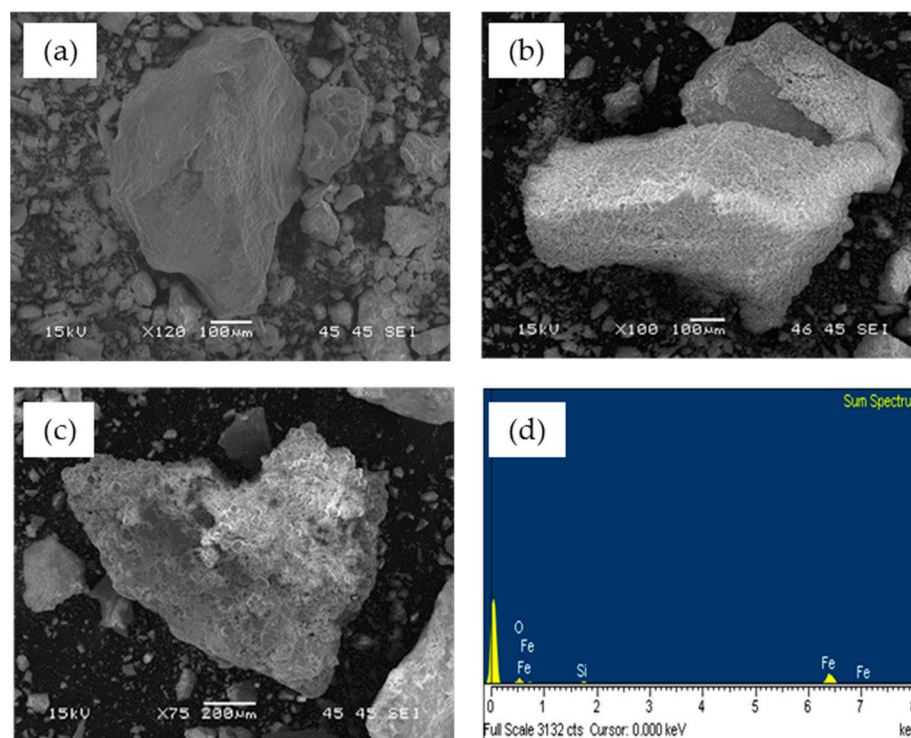


Figure 9. SEM microphotograph from solid at different leaching times: (a) 0 h, (b) 1 h, (c) 4 h. (d) EDS of sample at 4 h.

Then, diffusion of the reactant from the interface to the bulk of the host mineral containing rare earths takes place. Further, chemical reactions between the reactants and those in this mineral occur. Finally, the products diffuse into the bulk of the aqueous phase. However, the products of reactions are aqueous species, according to Equations (1)–(8). Then, reaction can proceed in a topochemical manner, in which the inner core of a REE

mineral decreases with time. In this case of low particle liberation or low porosity in inert mineral, the reaction products could be accumulated into porous of the inert material to form the named “product layer” around the reacting core. So, diffusion is the rate-limiting step of the reaction. But if the inert material is porous, or there is high particle liberation of La and Ce minerals, reactants and reaction products (both aqueous) diffuse into the solution without a layer that slows the reaction. In this case, chemical reaction is the rate-limiting step of rare earth leaching.

Therefore, to determine the rate-limiting step of the SCM model, the following equations are considered [35]:

(a) control by the chemical reaction:

$$kt = 1 - (1 - x)^{1/3} \tag{9}$$

where x is the fraction of REEs reacted; it can be calculated from the relationship between REE concentrations at the different time intervals with respect to initial concentration. k is the apparent rate constant.

(b) control by the diffusion of the reagents or dissolved species through the aqueous layer of reaction products. The fraction of REE reacted at any time t can be predicted from Equation (7):

$$kt = 1 - \frac{2}{3}x - (1 - x)^{2/3}. \tag{10}$$

The best adjustment model according to these kinetic models is SCM controlled by the chemical reaction. The obtained graphs show that the experimental data adjust to a straight line, given that the apparent rate constant will be determined.

Figure 10 shows the decreasing nucleus model versus time for phosphorus, calcium, iron, lanthanum, and cerium during leaching in a phosphoric acid medium.

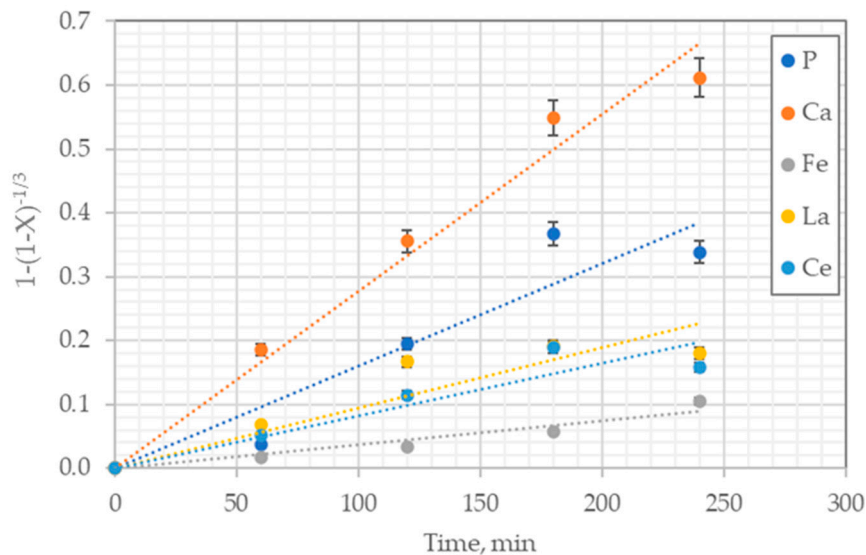


Figure 10. Shrinking model controlled by chemical reaction for leaching in phosphoric acid medium ($H_3PO_4 = 1\text{ M}$; $T = 40\text{ }^\circ\text{C}$; $S/L = 1/6$).

Figure 11 provides evidence that the kinetics adjust better to the experimental data for the leaching solution with hydrochloric acid, as this presents a significant approximation to the tendency line for the cases of lanthanum and cerium.

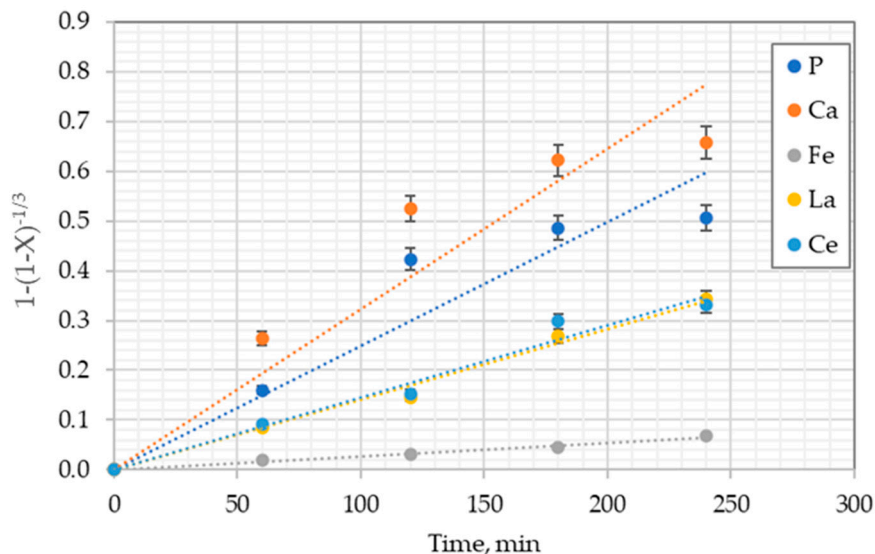


Figure 11. Shrinking model controlled by chemical reaction for leaching in hydrochloric acid medium (HCl = 1 M; T = 40 °C; S/L = 1/60).

To determine the activation energy and confirm that the leaching reaction of Ce and La is governed by the chemical reaction stage, the kinetic constants were determined at temperatures of 10, 20, 40, and 60 °C. For this analysis, only leaching with HCl was conducted, considering that it is the medium in which the best extraction percentages were obtained. Figure 12 shows the leaching of Ce and La at the different temperatures mentioned. The behavior of the two rare earths was similar, confirming that both are found as phosphates and react in a similar way with the acidic medium. In both cases, as the temperature increased, the extraction percentage increased. And at each temperature, as time passed, the amount of the leached component also increased. However, it was also observed that the percentage of extraction of both rare earths between the temperatures of 40 and 60 °C no longer increased proportionally.

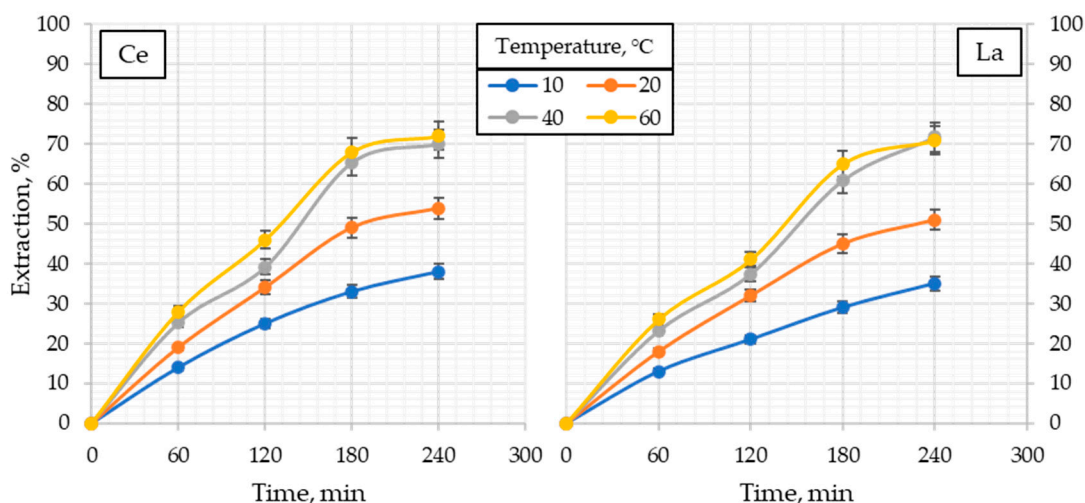


Figure 12. Leaching in a hydrochloric acid medium (HCl = 1 M; S/L = 1/60) at different temperatures.

Kinetics apparent rate constants calculated from the shrinking model controlled by a chemical reaction at different temperatures were used to calculate activation energy (E_a). The plot of $\ln k$ against $1/T$ (Figure 13) offers a straight line with a slope of $-E_a/R$ and the intercept of $\ln k$, according to a linearized Arrhenius equation [37]:

$$\ln k = \ln A - \left(\frac{E_a}{RT} \right) \tag{11}$$

where k is the apparent rate constant, A is the pre-exponential factor, R is the universal gas constant, and T is the absolute temperature.

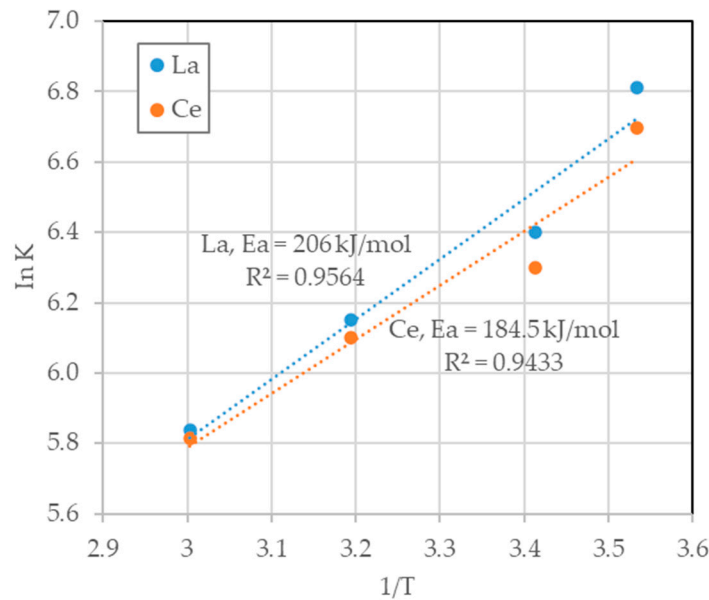


Figure 13. Activation energies obtained from the linearized Arrhenius equation.

The estimated activation energies from the slope were 205.84 and 184.5 kJ/mol for La and Ce, respectively. According to Habashi (1999), a chemically controlled process is usually greater than 10 kcal/mol (41.8 kJ/mol) [35]. The magnitude of the activation energies clearly confirms that the leaching of La and Ce in a HCl 1 M solution is most likely controlled by a chemical reaction.

As mentioned above, the rate of dissolution of an element or a compound and the model that represents its dissolution depend on many factors that do not allow for comparisons to be drawn. Table 3 shows some kinetic studies of REE leaching. The most used kinetic model is the SCM, regardless of the type of material that contains the REE and the experimental conditions. In most cases, the limiting stage encountered is diffusion in the product layer. In this sense, formation of solid products is assumed.

Table 3. Kinetic models and apparent activation energies reported in the literature.

Material	Conditions	Kinetic Model	Apparent Activation Energy	Ref.
REE in Polishing Powder Waste	HCl, 2 M; S/L ratio, 1/4	Shrinking core model; Control: interfacial transfer and product layer diffusion (La) and product layer diffusion (Ce), respectively	La and Ce leaching, 89.97 kJ/mol and 79.03 kJ/mol, respectively	[39]
REE from Phosphogypsum	HCl, 1.65 M; S/L ratio, 1/10	Shrinking core model; Reaction rate controlled by the interfacial transfer and diffusion across the product layer	For Σ REE leaching, 20.65 kJ/mol	[40]
REE from Phosphate Rock	H ₃ PO ₄ , 30%; S/L ratio, 1/12	Shrinking core model; Fast stage controlled by solid product layer diffusion; Slow stage controlled by chemical reaction and solid product layer diffusion	REE leaching, 11.22 kJ/mol (fast stage). 6.99–10.74 kJ/mol (slow stage)	[41]

Table 3. Cont.

Material	Conditions	Kinetic Model	Apparent Activation Energy	Ref.
Zircon tailings containing REE	HCl, 2 M; S/L ratio, 1/10	Zhuravlev–Leshokin–Templeman model	Light rare earth element leaching, 25.31 kJ/mol	[42]
REE from fire clay seam	Sulfuric acid	Shrinking core model: Chemical reaction control followed by the formation of a product layer	27–36 kJ/mol	[43]
REE in slag	H ₂ SO ₄ , 0.3 M S/L ratio, 1/67	Shrinking core model: Diffusion through an ash layer	24.8 kJ/mol	[44]
This study	HCl, 1 M; S/L ratio, 1/6	Shrinking core model: Chemical reaction control	205.84 and 184.5 kJ/mol for La and Ce, respectively	

In our case, the chemical reactions presented in Equations (1)–(6) (and supported by predominance diagrams, Figures 5 and 6) show the formation of aqueous products. So, the diffusion could occur through a liquid layer. However, the presence of good agitation conditions and a relatively high volume of solution with respect to the solid component facilitates, in both conditions, diffusion, so the limiting stage is the chemical reaction. This is in agreement with the apparent activation energy values obtained in this study.

4. Conclusions

The presence of La and Ce in ferrocarnatite-type minerals (from the north of Mexico) was determined. These rare earth elements appear in the form of phosphates, mainly as monazite associated with apatite.

These phosphates dissolve in an acid medium the efficiency of which depends on the type of acid and its concentration. The results indicated that the greatest dissolution is obtained using 1 M HCl and 2.3 M H₃PO₄. The species resulting from the leaching were determined thermodynamically using the predominance diagrams of the resulting species.

The extraction of La and Ce by leaching with HCl and H₃PO₄ is associated with the dissolution of apatite, given the high dissolution of calcium and phosphorus, which corroborates the notion that rare earth elements are also present as phosphates. The percentage of dissolution obtained also indicates that there was good liberation of the mineral that contains these rare earths at a particle size of less than 150 microns.

Iron dissolution was lower when using HCl (20%) than when using H₃PO₄ (almost 30%). This is important to highlight given that the mineral is rich in this element. High concentrations of iron in the solution result in greater difficulties in the recovery of rare earths.

For kinetics, only leaching with HCl was evaluated, as it had better results when compared with H₃PO₄ at the same initial concentration (1 M). The results indicated that the leaching kinetics follow the SCM model and that the limiting step is the chemical reaction, according to the activation energy values obtained.

Author Contributions: Conceptualization, F.R.C.-P.; methodology, M.d.J.S.-A. and A.M.-L.; software, N.G.P.-R.; characterization, U.F.-L. and M.d.J.S.-A.; formal analysis, D.A.T.-S. and F.R.C.-P.; investigation, D.A.T.-S.; resources, F.R.C.-P.; writing—original draft preparation, N.G.P.-R. and F.R.C.-P.; writing—review and editing, J.L.V.G. and A.M.-L.; project administration, F.R.C.-P. and A.M.-L. All authors have read and agreed to the published version of the manuscript.

Funding: This research received no external funding.

Data Availability Statement: The raw data supporting the conclusions of this article will be made available by the authors on request.

Acknowledgments: The authors thank CONAHCyT for scholarship No. 887854, the Doctorate in Materials Science and Technology of the Faculty of Chemical Sciences, and the Faculty of Metallurgy (both of the Autonomous University of Coahuila).

Conflicts of Interest: The authors declare no conflicts of interest.

References

1. Ford, A.; Huston, D.; Cloutier, J.; Doublier, M.; Schofield, A.; Cheng, Y.; Beyer, E. A national scale mineral potential assessment for carbonatite-related rare earth element mineral systems in Australia. *Ore Geol. Rev.* **2023**, *161*, 105658. [\[CrossRef\]](#)
2. Du, X.; Graedel, T.E. Global in-use stocks of the rare earth elements: A first estimate. *Environ. Sci. Technol.* **2011**, *45*, 4096–4101. [\[CrossRef\]](#)
3. Zhou, B.; Li, Z.; Chen, C. Global potential of rare earth resources and demand for rare earths from clean technologies. *Minerals* **2017**, *7*, 203. [\[CrossRef\]](#)
4. Wang, Z.-Y.; Fan, H.-R.; Zhou, L.; Yang, K.-F.; She, H.-D. Carbonatite-Related REE Deposits: An Overview. *Minerals* **2020**, *10*, 965. [\[CrossRef\]](#)
5. Negeri, T. Flotation-Calcination-Magnetic Separation Hybrid Process for Concentration of Rare Earth Minerals Contained in a Carbonatite Ore. *J. Miner. Mater. Charact. Eng.* **2021**, *9*, 271–289. [\[CrossRef\]](#)
6. Yang, J.; Song, W.; Liu, Y.; Zhu, X.; Kynicky, J.; Chen, Q. Mineralogy and element geochemistry of the Bayan Obo (China) carbonatite dykes: Implications for REE mineralization. *Ore Geol. Rev.* **2024**, *165*, 105873. [\[CrossRef\]](#)
7. Prokopyev, I.; Borisenko, A.; Borovikov, A.; Pavlova, G. Origin of REE-rich ferrocarnatites in southern Siberia (Russia): Implications based on melt and fluid inclusions. *Miner. Petrol.* **2016**, *110*, 845–859. [\[CrossRef\]](#)
8. Gittins, J.; Harmer, R. What is ferrocarnatite? A revised classification. *J. Afr. Earth Sci.* **1997**, *25*, 159–168. [\[CrossRef\]](#)
9. Chen, S.; Zhao, L.; Wang, M.; Feng, Z.; Xia, C.; Xu, Y.; Huang, X. Effects of iron and temperature on solubility of light rare earth sulfates in multicomponent system of $\text{Fe}_2(\text{SO}_4)_3\text{-H}_3\text{PO}_4\text{-H}_2\text{SO}_4$ synthetic solution. *J. Rare Earths* **2020**, *38*, 1243–1250. [\[CrossRef\]](#)
10. Long, K.R.; van Gosen, B.S.; Foley, N.K.; Cordier, D. *The Principle Rare Earth Elements Deposits of the United States—A Summary of Domestic Deposits and a Global Perspective*; Scientific Investigations Report 2010-5220; U.S. Geological Survey: Reston, VA, USA, 2010.
11. Chen, L.; He, X.; Dang, X.; Wang, X.; Liu, W.; Zhang, D.; Yang, T. Rare earth dissolution from polishing powder waste in $\text{H}_2\text{O}_2\text{-H}_2\text{SO}_4$ system: Condition optimization and leaching mechanism. *Hydrometallurgy* **2024**, *224*, 106248. [\[CrossRef\]](#)
12. Balinski, A.; Atanasova, P.; Wiche, O.; Kelly, N.; Reuter, M.; Scharf, C. Recovery of REEs, Zr(+Hf), Mn and Nb by H_2SO_4 leaching of eudialyte concentrate. *Hydrometallurgy* **2019**, *186*, 176–186. [\[CrossRef\]](#)
13. Tang, M.; Zhou, C.; Pan, J.; Zhang, N.; Liu, C.; Cao, S.; Hu, T.; Ji, W. Study on extraction of rare earth elements from coal fly ash through alkali fusion—Acid leaching. *Miner. Eng.* **2019**, *136*, 36–42. [\[CrossRef\]](#)
14. Chen, X.; Guo, F.; Chen, Q.; Liu, X.; Zhao, Z. Leaching tungsten and rare earth elements from scheelite through $\text{H}_2\text{SO}_4\text{-H}_3\text{PO}_4$ mixed acid decomposition. *Miner. Eng.* **2020**, *156*, 106526. [\[CrossRef\]](#)
15. Innocenzi, V.; Veglio, F. Recovery of rare earths and base metals from spent nickel-metal hydride batteries by sequential sulfuric acid leaching and selective precipitations. *J. Power Sources* **2012**, *211*, 184–191. [\[CrossRef\]](#)
16. Kim, R.; Cho, H.; Han, K.N.; Kim, K.; Mun, M. Optimization of acid leaching of rare-earth elements from Mongolian apatite-based ore. *Minerals* **2016**, *6*, 63. [\[CrossRef\]](#)
17. Shen, Y.; Jiang, Y.; Qiu, X.; Zhao, S. Leaching of Light Rare Earth Elements from Sichuan Bastnaesite: A Facile Process to Leach Trivalent Rare Earth Elements Selectively from Tetravalent Cerium. *JOM* **2017**, *69*, 1976–1981. [\[CrossRef\]](#)
18. Xu, D.; Shah, Z.; Cui, Y.; Jin, L.; Peng, X.; Zhang, H.; Sun, G. Recovery of rare earths from nitric acid leach solutions of phosphate ores using solvent extraction with a new amide extractant (TODGA). *Hydrometallurgy* **2018**, *180*, 132–138. [\[CrossRef\]](#)
19. Liu, F.; Porvali, A.; Halli, P.; Wilson, B.P.; Lundström, M. Comparison of Different Leaching Media and Their Effect on REEs Recovery from Spent Nd-Fe-B Magnets. *JOM* **2020**, *72*, 806–815. [\[CrossRef\]](#)
20. Echeverry-Vargas, L.; Ocampo-Carmona, L.M. Recovery of Rare Earth Elements from Mining Tailings: A Case Study for Generating Wealth from Waste. *Minerals* **2022**, *12*, 948. [\[CrossRef\]](#)
21. Chakhmouradian, A.R.; Wall, F. Rare earth elements: Minerals, mines, magnets (and more). *Elements* **2012**, *8*, 333–340. [\[CrossRef\]](#)
22. Masmoudi-Soussi, A.; Hammas-Nasri, I.; Horchani-Naifer, K.; Ferid, M. Rare earths recovery by fractional precipitation from a sulfuric leach liquor obtained after phosphogypsum processing. *Hydrometallurgy* **2020**, *191*, 105253. [\[CrossRef\]](#)
23. McLemore, V.T. Great Plains Margin (alkaline-related) gold deposits in New Mexico: Twenty years later. In *New Concepts and Discoveries, 2015 Symposium Volume*; Geological Society of Nevada: Reno/Sparks, NV, USA, 2015; Volume II, pp. 1305–1328.
24. Laurino, J.P.; Mustacato, J.; Huba, Z.J. Rare earth element recovery from acidic extracts of Florida phosphate mining materials using chelating polymer 1-octadecene, polymer with 2,5-furandione sodium salt. *Minerals* **2019**, *9*, 477. [\[CrossRef\]](#)
25. Lambert, A.; Anawati, J.; Walawalkar, M.; Tam, J.; Azimi, G. Innovative application of microwave treatment for recovering of rare earth elements from phosphogypsum. *ACS Sustain. Chem. Eng.* **2018**, *6*, 16471–16481. [\[CrossRef\]](#)
26. Brückner, L.; Elwert, T.; Schirmer, T. Extraction of rare earth elements from phosphogypsum: Concentrate digestion, leaching, and purification. *Metals* **2020**, *10*, 131. [\[CrossRef\]](#)
27. Grabas, K.; Pawelczyk, A.; Strek, W.; Szeleg, E.; Strek, S. Study on the properties of waste apatite phosphogypsum as a material of prospective application. *Waste Biomass Valoriz.* **2019**, *10*, 3143–3155. [\[CrossRef\]](#)
28. Virolainen, S.; Repo, E.; Sainio, T. Recovering rare earth elements from phosphogypsum using a resin-in-leach process: Selection of resin, leaching agent, and eluent. *Hydrometallurgy* **2019**, *189*, 105125. [\[CrossRef\]](#)
29. Rychkov, V.N.; Kirillov, E.V.; Kirillov, S.V.; Semenishchev, V.S.; Bunkov, G.M.; Botalov, M.S.; Smyshlyaev, D.V.; Malyshev, A.S. Recovery of rare earth elements from phosphogypsum. *J. Clean. Prod.* **2018**, *196*, 674–681. [\[CrossRef\]](#)

30. Hammas-Nasri, I.; Horchani-Naifer, K.; Férid, M.; Barca, D. Rare earths concentration from phosphogypsum waste by two-step leaching method. *Int. J. Miner. Process.* **2016**, *149*, 78–83. [[CrossRef](#)]
31. Walawalkar, M.; Nichol, C.K.; Gisele Azimi, G. Process investigation of the acid leaching of rare earth elements from phosphogypsum using HCl, HNO₃ and H₂SO₄. *Hydrometallurgy* **2016**, *166*, 195–204. [[CrossRef](#)]
32. Al-Thyabat, S.; Zhang, P. REE extraction from phosphoric acid, phosphoric acid sludge, and phosphogypsum. *Miner. Proc. Extr. Metall.* **2015**, *124*, 143–150. [[CrossRef](#)]
33. Ismail, Z.; Abu Elgoud, E.; Gasser, M.; Aly, H.; Abdel Hai, F.; Ali, I. Leaching of some lanthanides from phosphogypsum fertilizers by mineral acids. *Arab J. Nucl. Sci. Appl.* **2015**, *48*, 37–50.
34. Gasser, M.S.; Ismail, Z.H.; Abu Elgoud, A.; Abdel Hai, F.; Ali, O.I.; Aly, H.F. Process for lanthanides-Y leaching from phosphogypsum fertilizers using weak acids. *J. Hazard. Mater.* **2019**, *378*, 12762. [[CrossRef](#)]
35. Du, A.; Jarfors, A.E.W.; Zheng, J.; Wang, K.; Yu, G. The influence of La and Ce on microstructure and mechanical properties of an Al-Si-Cu-Mg-Fe Alloy at high temperature. *Metals* **2021**, *11*, 384. [[CrossRef](#)]
36. Sims, Z.; Kesler, M.; Henderson, H. How Cerium and Lanthanum as coproducts promote stable rare earth production and new alloys. *J. Sustain. Metall.* **2021**, *8*, 1225–1234. [[CrossRef](#)]
37. Habashi, F. *Kinetics of Metallurgical Process*; Métallurgie Extractive: Québec City, QC, Canada, 1999.
38. Faraji, F.; Alizadeh, A.; Rashchi, F.; Mostoufi, N. Kinetics of leaching: A review. *Rev. Chem. Eng.* **2022**, *38*, 113–148. [[CrossRef](#)]
39. Li, Y.; Yang, F.; Xiong, J.; Liu, K.; Xiao, W.; Qi, T.; Dong, Z.; Wang, Y. Separation of La/Ce in rare earth polishing powder waste via Two-Stage hydrochloric acid leaching and corresponding leaching mechanism. *Sep. Purif. Technol.* **2024**, *330*, 125297. [[CrossRef](#)]
40. Guan, Q.; Sui, Y.; Liu, C.; Wang, Y.; Zeng, C.; Yu, W.; Chi, R. Characterization and leaching kinetics of rare earth elements from phosphogypsum in hydrochloric acid. *Minerals* **2022**, *12*, 703. [[CrossRef](#)]
41. Li, Z.; Xie, Z.; Deng, J.; He, D.; Zhao, H.; Liang, H. Leaching kinetics of rare earth elements in phosphoric acid from phosphate rock. *Metals* **2021**, *11*, 239. [[CrossRef](#)]
42. Prameswara, G.; Trisnawati, I.; Mulyono, P. Leaching behaviour and kinetic of light and heavy rare earth elements (REE) from zircon tailings in Indonesia. *JOM* **2021**, *73*, 988–998. [[CrossRef](#)]
43. Yang, X.; Honaker, R.Q. Leaching kinetics of rare earth elements from fire clay seam coal. *Minerals* **2020**, *10*, 491. [[CrossRef](#)]
44. Kim, C.J.; Yoon, H.S.; Chung, K.W.; Lee, J.Y.; Kim, S.D.; Shin, S.M.; Lee, S.J.; Joe, A.R.; Lee, S.I.; Kim, S.H.; et al. Leaching kinetics of lanthanum in sulfuric acid from rare earth element (REE) slag. *Hydrometallurgy* **2014**, *146*, 133–137. [[CrossRef](#)]

Disclaimer/Publisher's Note: The statements, opinions and data contained in all publications are solely those of the individual author(s) and contributor(s) and not of MDPI and/or the editor(s). MDPI and/or the editor(s) disclaim responsibility for any injury to people or property resulting from any ideas, methods, instructions or products referred to in the content.